Conf-930173--9

BNL-48649

Neutral Strange Particle Production at the AGS *

S.E. Eiseman, A. Etkin, K.J. Foley, R.W. Hackenburg, R.S. Longacre, W.A. Love

T.W. Morris, E.D. Platner and A.C. Saulys

Brookhaven National Laboratory, Upton, NY 11973, USA

S.J. Lindenbaum

Brookhaven National Laboratory, Upton, NY 11973, USA

and City College of New York, NY 10031, USA

C.S. Chan, E. Efstathiadis, M.A. Kramer, K. Zhao and Y. Zhu

City College of New York, NY 10031, USA

T.J. Hallman,† L. Madansky

Johns Hopkins University, Baltimore, MD 21218, USA

S. Ahmad, B.E. Bonner, J.A. Buchanan, C.N. Chiou, J.M. Clement and G.S. Mutchler

Rice University, Houston, TX 77251, USA

Paper submitted to:

Proceedings of HIPAGS93

February 11, 1993

* This research was supported by the U.S. Department of Energy under Contract Nos. DE-AC02-76CH00016, DE-FG02-91ER40645, DE-FG02-88ER40413 and DE-FG05- 87ER40309, and the City University of New York PSC-BHE Research Award Program.

† Present address: University of California, Los Angeles, CA 90024, USA

NEUTRAL STRANGE PARTICLE PRODUCTION AT THE AGS

ALFRED C. SAULYS
Brookhaven National Laboratory Upton, NY 11973, USA

for the E810 Collaboration:

S.E. Eiseman, A. Etkin, K.J. Foley, R.W. Hackenburg, R.S. Longacre, W.A. Love
T.W. Morris, E.D. Platner and A.C. Saulys
Brookhaven National Laboratory, Upton, NY 11973, USA

S.J. Lindenbaum
Brookhaven National Laboratory, Upton, NY 11973, USA
and City College of New York, NY 10031, USA

C.S. Chan, E. Efstathiadis, M.A. Kramer, K. Zhao and Y. Zhu
City College of New York, NY 10031, USA

T.J. Hallman,† L. Madansky
Johns Hopkins University, Baltimore, MD 21218, USA

S. Ahmad, B.E. Bonner, J.A. Buchanan, C.N. Chiou, J.M. Clement and G.S. Mutchler
Rice University, Houston, TX 77251, USA

ABSTRACT

We present the results of Λ and K^0_s production from *Si* and *Pb* targets with 14.6×A Gev/c *Si* beams. The measured rapidity distributions and the transverse mass exponential slopes are presented and compared with models.

1. Introduction

There is considerable interest in studying strange particle production in heavy ion interactions, since enhancement of strangeness production over that expected from a superposition of nucleon-nucleon interactions has been reported by several experiments.[1,2,3] Strange particles contain quarks that have to be produced in the interaction. The understanding of their production characteristics may be a better probe of the reaction mechanism than the study of produced particles which are made up of the quarks in the nucleons forming the original interacting nuclei. Enhanced strange particle production in heavy ion interactions has been suggested as one of the signals of quark-gluon plasma (QGP) formation[4]. An enhancement in itself cannot be considered as a signal for QGP formation, but unusual characteristics of the strange particle production distributions in correlation with other signals may be strong evidence for QGP formation. Our measurements of these distributions place a tight

†Present address: University of California, Los Angeles, CA 90024, USA

restriction on conventional cascade model calculations which predict the distributions of all particles produced in heavy ion interactions.

2. Experimental method

The experimental method was described in previous publications[5,6]. Briefly, experiment E810 measured charged tracks in three TPC (Time Projection Chamber) modules in a magnetic field. The detector covered the forward hemisphere in the center-of-mass. The trigger, as described in Ref. 5, selected centrally enriched events for data recording. For the final data sample we selected the most central events using a cut on the highest multiplicity of the negatively charged tracks within our good acceptance. We found this to be a reasonably good measure of the centrality from both the increased yield of K^0_s's and Λ's as a function of this multiplicity[5] and from Monte Carlo studies of the correlation of impact parameter with this multiplicity. We selected the most central events from the *Si* target corresponding to a cross section of approximately 100 mb, and for *Pb* corresponding to a cross section of approximately 300 mb. These cuts correspond to approximately 10% of the geometric cross section. Since we have shown in Ref. 5 that the yield of Λ's and K^0_s's is linearly dependent on our centrality selection criterion (negative multiplicity), any tighter cut for centrality selection is not justified because of limited statistics and our estimated systematic error of 20%. Thin targets were used to reduce γ ray conversion which would give incorrect hadron multiplicities. We used a 0.122 cm thick *Si* target (1.3% radiation length) and a 0.02 cm thick *Pb* target (3.5% radiation length). For more details on the experimental method see Refs. 5 and 6. The effective masses for K^0_s's and Λ's were calculated by kinematic hypothesis by assigning a proton or a pion mass to the charged tracks which form a vertex away from the point of interaction (see Ref. 6 for more details).

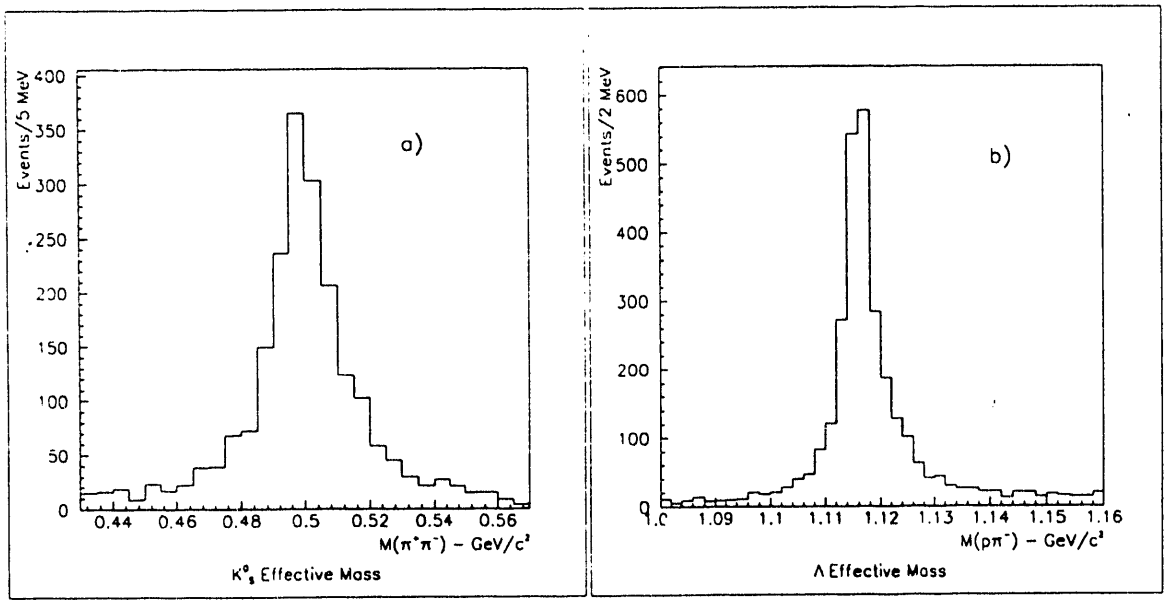

Fig. 1: (a). Effective mass plot of the $\pi^+\pi^-$ hypothesis for decay vertices from *Pb* target with vertices removed if they satisfy the Λ effective mass cuts. (b) Effective mass plot of the proton π^- hypothesis for decay vertices from *Pb* target.

Figure Fig. 1a shows the result of the effective mass calculation for the $\pi^-\pi^+$ hypothesis and Fig. 1b shows the result of the proton π^- hypothesis for our final selected data sample from the Pb target. Decay vertices with effective masses in the range of 0.475-0.525 GeV/c^2 were selected as K^0_s's and those in the range of 1.106-1.126 GeV/c^2 were selected as Λ's. As can be seen, the K^0_s and Λ signals are quite evident and the backgrounds are relatively small (<10%). In all cases the tails of the effective mass distributions were used for background subtractions.

We have also calculated the effective mass distribution for the anti-proton π^+ hypothesis. We do not see any statistically significant $\bar{\Lambda}$ signal. We obtain an upper limit of $\bar{\Lambda}/\Lambda <$ 1% (95% CL) for both Si and Pb targets.

3. Results

In this report we present the results of 817 K^0_s's produced from a Si target with rapidities $2.0 < y < 3.5$ and 2241 K^0_s's from Pb target with rapidities $1.7 < y < 3.5$. We also present the results of 1122 Λ's from Si target and 3060 Λ's from Pb target, both in the rapidity range of $1.4 < y < 3.2$. The rapidity distributions from the Si target have been published[6]. Here we present exponential transvere mass slopes and a higher statistics data sample from the Pb target.

Most experiments measure relevant variables within a finite aperture and so do we. In order to extrapolate to unmeasured regions of the transverse momentum p_t we have fitted our acceptance corrected data to

$$1/m_t \cdot d^2N/dydm_t = A \exp(-Bm_t), \tag{1}$$

where

$$m_t = \sqrt{p_t^2 + m_0^2}. \tag{2}$$

We could present rapidity distributions integrated only over our measured transverse momentum range of $p_t < 1.0$ GeV/c, but this makes it difficult to compare our measurements with other experiments. In either case the corrections for exponential extrapolation for values of $p_t > 1.0$ GeV/c are of the order of 10% for K^0_s's and 25% for Λ's. We have performed the fit under two hypotheses: 1) A is an arbitrary constant determined at each rapidity bin and B is a constant independent of rapidity; and 2) A is an arbitrary constant independent of rapidity and B takes the form of $B = a + b\,cosh(y - y_0)$ where a and b are independent of rapidity. The motivation for the second hypothesis is the fireball model[7]. The inverse slope of the exponential is usually called the temperature of the fireball. The fit was done in a 6×7 grid in y and m_t space for $p_t < 1.0$ GeV/c and in the above mentioned rapidity ranges. The χ^2 probabilities for the fits for the two hypotheses are shown in Table 1. In all cases, except for Λ's from Si target, the χ^2 probability is better for the fit including the $cosh(y - y_0)$ term (the second hypothesis). The reason both hypotheses satisfy the Λ's from the Si target is due to low statistics. The second hypothesis is clearly an acceptable representation of our data. We use it for extracting results from our data.

It is interesting to compare the total yields of K^0_s and Λ's in the rapidity region accessible to our apparatus (basically the forward hemisphere in the CM) with models. For our comparisons we have selected two models: ARC[9] and AGSHIJET+N*[10]. The second

Particle	Target	Constant slope $P(\chi^2)$	cosh(y) added $P(\chi^2)$
K^0_s	Si	8%	57%
K^0_s	Pb	<.01%	52%
Λ	Si	67%	66%
Λ	Pb	4%	22%

Table 1: χ^2 probabilities for the two fit hypotheses as explained in text.

	Target	Data	AGSHIJET+N*	ARC
K^0_s Yield/Central Event for $2.0 < y < 3.5$	Si	.5	.4	.6
	Pb	.7	.6	.9
Λ Yield/Central Event for $1.7 < y < 3.2$	Si	1.2	.6	1.3
	Pb	1.3	.8	1.2

Table 2: Integrated yields of K^0_s's and Λ's compared with two models. The statistical errors of the yields are small compared to the estimated systematic uncertainty of 20%.

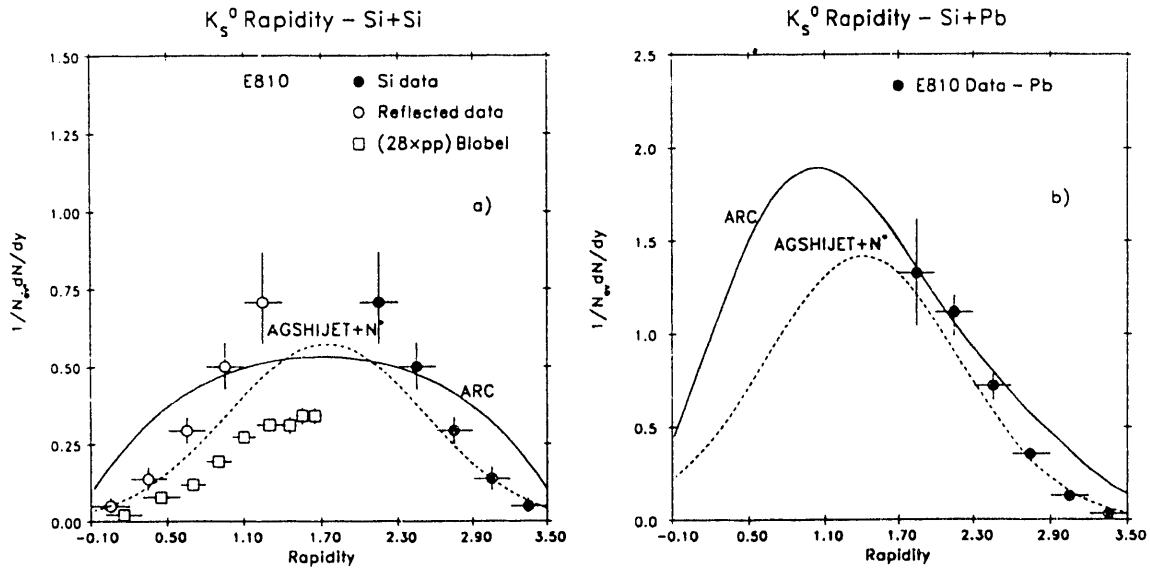

Fig. 2: (a) Rapidity distribution for K^0_s's from the Si target. The solid points above a rapidity of 1.7 are our measurements. Errors shown are statistical only. The open circles below rapidity of 1.7 are our measurements reflected about 1.7. The open squares represent the measurements of Ref. 8 scaled up by 28. The solid curve is the prediction of the ARC model. The dashed curve is the prediction of the HIJET with N^*'s included in the model. (b) Rapidity distribution for K^0_s's from the Pb target.

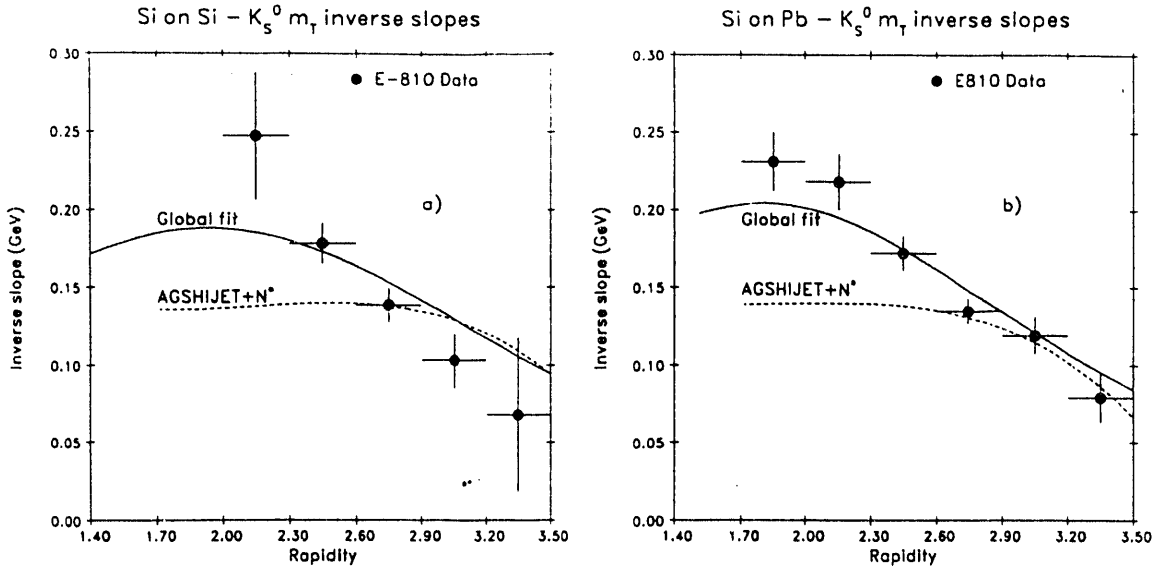

Fig. 3: (a) Inverse exponential slopes for K_s^0's from the *Si* target. The points are fits to an exponential in each rapidity bin. The solid curve is the result of our global fit, not a fit to the points. The statistical error on the curve representation is similar to that shown on the individual points. The dashed curve is the prediction of AGSHIJET+N*. (b) Inverse exponential slopes for K_s^0's from the *Pb* target.

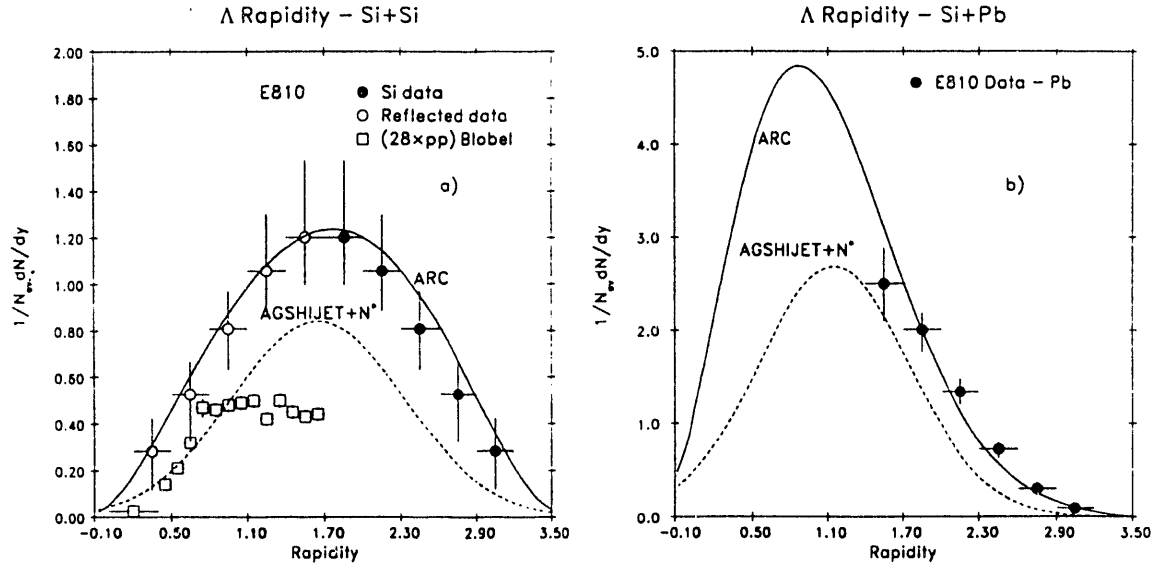

Fig. 4: (a) Rapidity distribution for Λ's from the *Si* target. The solid points above a rapidity of 1.7 are our measurements. Errors shown are tatistical only. The open squares represent the measurements of Ref [8] scaled up by 28. The solid curve is the prediction of the ARC model. The dashed curve is the prediction of the AGSHIJET+N* model. (b) Rapidity distribution for Λ's from the *Pb* target.

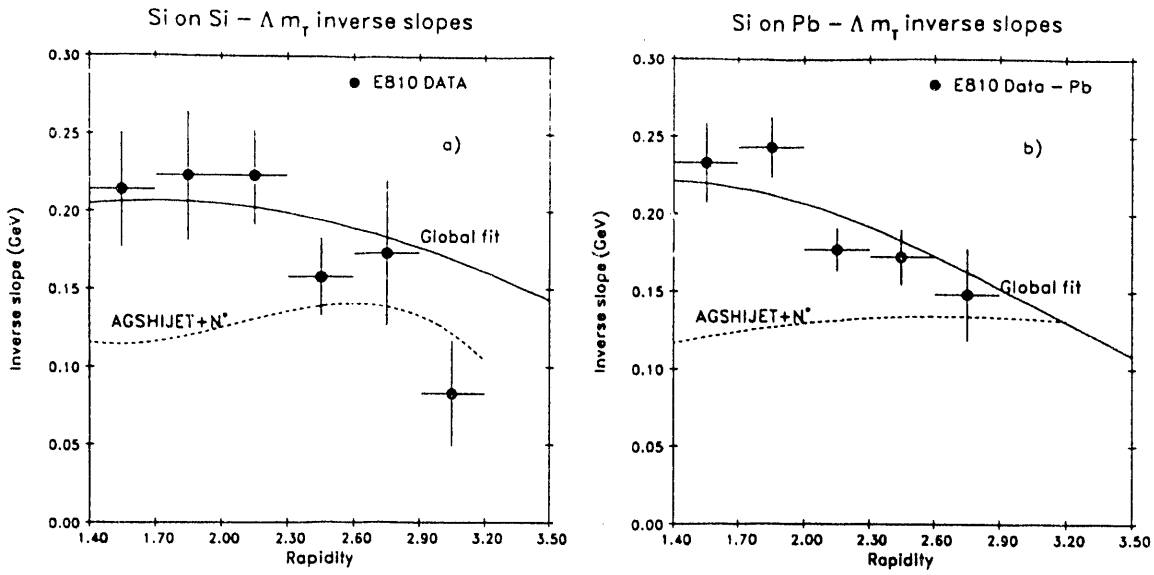

Fig. 5: (a) Inverse exponential slopes for Λ's from the *Si* target. The points are fits to an exponential in m_t for each rapidity bin. The solid curve is the result of our global fit, not a fit to the points. The statistical error on the curve representation is approximately as shown on the individual points. The dashed curve is the prediction of AGSHIJET+N*. (b) Inverse exponential slopes for Λ's from the *Pb* target.

model is well described in these proceedings[10]. The results of the comparison are shown in Table 2. The statistical errors on the data column are small, but we estimate an overall systematic error of 20%. The integrated K^0_s yields agree well with both the predictions of AGSHIJET+N* and ARC. The Λ yields are predicted well by ARC, but underestimated by AGSHIJET+N* by about a factor of 2. The integrated Λ yields in the rapidity region of $1.7 < y < 3.2$ are the same (within errors) from both *Si* and *Pb* targets. This would be a very misleading result if we did not measure the rapidity distributions, since they are very different for the two targets. This is just one example where it is important to measure and compare differential cross sections not just particle yields.

In Fig. 2 we plot the rapidity distributions for K^0_s's from *Si* and *Pb* targets. The curves shown in the figures are the predictions of the two models. Errors shown are statistical only and were calculated using a technique discussed in Ref. 6. Also shown on Fig. 2a are the measured rapidity distributions[8] for $p + p \Rightarrow K^0_s + X$ at 12 GeV/c scaled up by a factor of 28. The rapidity distributions for *Si* were measured only for forward rapidities, but reflected about $y = 1.7$ (corresponds to $\sim y = 0$ in the nucleon-nucleon c.m.s.) because of the symmetry of the reaction. In this way we obtain a measurement of the whole rapidity distribution. The *Si* target results have been previously published[6], but the *Pb* target data contains more data than shown in Ref. 6. The first thing to be noted is that our *Si* data cannot be described by the naive assumption that we can scale up the *pp* cross sections by 28. AGSHIJET+N* seems to do a reasonable job of predicting the K^0_s rapidity distributions for both the *Si* and *Pb* targets, especially at higer rapidities. ARC predicts a yield that is too big by about a factor of 2 at high rapidities. This discrepancy is a direct result of the *pp* data input into the cascade which at present achieves the correct overall level of strangeness production with too wide a rapidity distribution. This will be suitably adjusted in future

Category		ARC	AGSHIJET+N*
Yield/event	K_s^0	Yes	Yes
$(y > y_{mid})$	Λ	Yes	No
Shape of rapidity	K_s^0	No	Yes
distribution	Λ	Yes	No
m_t slope	K_s^0	?	No
	Λ	?	No

Table 3: Summary of data comparison with ARC and AGSHIJET+N* by category. Yes means agreement with our data.

versions of ARC (private communication from authors of Ref. 9).

Since our data are consistent with exponential dependence in transverse mass, we next show our results for the inverse slope for K_s^0 as a fuction of rapidity in Fig. 3. The first thing to note is that our data are consistent with the $cosh(y - y_0)$ dependence used in our global fit. The general behavior of the inverse slopes is a value of $\sim$ 200 MeV at mid-rapidity dropping off to $\sim$ 100 MeV at high rapidities for both the Si and Pb targets. AGSHIJET+N* predicts a consistently lower inverse slope at mid-rapidity for both Si and Pb targets. The predictions from ARC are unavailable.

In Fig. 4 we plot the rapidity distributions of Λ's from Si and Pb targets. Again the points and the curves represent the data and the models in the same way as for the K_s^0 rapidity distributions. The ARC predictions are in excellent agreement with the data for both the Si and Pb targets. AGSHIJET+N* underestimates the yield for both targets.

In Fig. 5 we plot the inverse of exponential slopes for Λ's produced from Si and Pb targets. Unfortunately, because of kinematics, for the same transverse momentum range we cover a smaller range in transverse mass making it more difficult to measure the exponential slopes. This fact is reflected in the larger errors, although the general picture is similar to that of the K_s^0's. The inverse slopes are $\sim$ 200 MeV at mid-rapidity decreasing to $\sim$ 100 – 150 MeV at high rapidities for both the Si and Pb targets. Again AGSHIJET+N* predicts lower inverse slopes than observed. The predictions of ARC are unavailable.

4. Summary and conclusions

In Table 3 we show a summary of data comparison with the AGSHIJET+N* and ARC model predictions by category. It points out the obvious necessity to compare differential cross sections with model predictions instead of just particle yields. In order to find new phenomena in relativistic heavy ion interactions we need detailed model predictions based on observed nucleon-nucleon cross section measurements so that we know that the deviations from the model predictions could be interperted as new phenomena, such as QGP formation.

Our K_s^0 data are inconsistent with a constant exponential transverse mass slope as a function of rapidity for both Si and Pb targets. The data favors the slope behavior of $B = a + b \times cosh(y - y_0)$. Our Λ data are also consistent with $cosh(y - y_0)$ rapidity dependence of the slope.

In conclusion, we can see at this point in time that ARC and AGSHIJET+N* do not explain all the features of our data. Whether refinements in the models will eventually explain all the features for all the particles produced in relativistic heavy ion interactions only time will tell.

5. Acknowledgements

We wish to thank the members of the AGS and MPS staff for their support during this experiment. Our special thanks go to E. Mogavero for help during the data analysis.

This research was supported by the U.S. Department of Energy under Contract Nos. DE-AC02-76CH00016, DE-FG02-91ER40645, DE-FG02-88ER40413 and DE-FG05- 87ER40309, and the City University of New York PSC-BHE Research Award Program.

6. References

1. T. Abbott *et al.*, Phys. Rev. Lett. 64 (1990) 847; T. Abbott *et al.*, Phys. Rev. Lett. 66 (1991) 1567.
2. J. Bartke *et al.*, Z. Phys. C48 (1990) 191. S. Abatzis *et al.*, Phys. Lett. B244 (1990) 130;
3. S. Abatzis *et al.*, Phys. Lett. B259 (1991) 508; S. Abatzis *et al.*, Phys. Lett. B270 (1991) 123.
4. J. Rafelski and R. Hagedorn, in: Thermodynamics of quarks and hadrons, ed. H. Satz (North-Holland, Amsterdam, 1981).
5. S.E. Eiseman *et al.*, Phys. Lett. B248 (1990) 254.
6. S.E. Eiseman *et al.*, Phys. Lett. B297 (1992) 44-48.
7. A. Bamberger *et al.*, Z. Phys. C38 (1988) 89; J. Stachel, Formation and Break-up of Hadronic Fireballs, in: Proc. of the Workshop on Heavy Ions at the AGS, (Brookhaven National Laboratory, March 1990), ed. O. Hansen, BNL-44911 (1990) 144.
8. V. Blobel *et al.*, Nucl. Phys. B69 (1974) 454.
9. Y. Pang, T.J. Schlagel, and S.H. Kahana, Phys. Rev. Lett. 68 (1992) 2743.
10. R. Longacre, HIJET with AGS Physics and N*'s, in these Proceedings.

END

DATE
FILMED
7/19/93